Pharmaceutical Research, Vol. 26, No. 6, June 2009 (© 2009)
DOI: 10.1007/s11095-009-9854-x

Research Paper

Effects of Ionic Strength on Passive and Iontophoretic Transport of Cationic Permeant Across Human Nail

Kelly A. Smith,[1] Jinsong Hao,[1] and S. Kevin Li[1,2]

Received October 14, 2008; accepted February 9, 2009; published online March 7, 2009

Purpose. Transport across the human nail under hydration can be modeled as hindered transport across aqueous pore pathways. As such, nail permselectivity to charged species can be manipulated by changing the ionic strength of the system in transungual delivery to treat nail diseases. The present study investigated the effects of ionic strength upon transungual passive and iontophoretic transport.
Methods. Transungual passive and anodal iontophoretic transport experiments of tetraethylammonium ion (TEA) were conducted under symmetric conditions in which the donor and receiver had the same ionic strength *in vitro*. Experiments under asymmetric conditions were performed to mimic the *in vivo* conditions. Prior to the transport studies, TEA uptake studies were performed to assess the partitioning of TEA into the nail.
Results. Permselectivity towards TEA was inversely related to ionic strength in both passive and iontophoretic transport. The permeability and transference number of TEA were higher at lower ionic strengths under the symmetric conditions due to increased partitioning of TEA into the nail. Transference numbers were smaller under the asymmetric conditions compared with their symmetric counterparts.
Conclusions. The results demonstrate significant ionic strength effects upon the partitioning and transport of a cationic permeant in transungual transport, which may be instrumental in the development of transungual delivery systems.

KEY WORDS: charge–charge interactions; human nail; ionic strength; iontophoresis; partition coefficient.

INTRODUCTION

As a result of its composition—80% protein, 7–12% water, less than 1.5% lipid, and trace amounts of minerals and electrolytes—the human nail plate acts as a robust barrier (1–7). Specifically, the nail behaves as a hydrophilic matrix resistant to penetration of large and lipophilic molecules such as antifungal agents (8–15). Only two drugs ciclopirox (Penlac®) and amorolfine (Loceryl®) are delivered topically into and across the nail in the treatment of onychomycosis, the most commonly diagnosed dermatological nail disorder. All other antifungal medications, including griseofulvin (Grisactin®), itraconazole (Sporanox®), ketoconazole (Nizarol®), terbinafine (Lamisil®), and off-label fluconazole (Diflucan®), are administered orally with the risk of adverse effects like liver damage and drug–drug interactions (16).

In addition to the barrier properties of the nail, the delivery of antifungal drugs across the nail is also hampered by the physicochemical properties of the drugs. The available antifungal drugs are highly hydrophobic as evidenced in their octanol–water partition coefficients (17). As such, they exhibit poor aqueous solubilities and nail permeability. Increasing their aqueous solubilities seems critical in developing a transungual iontophoretic delivery system. Organic solvents may be used in formulating these drugs but these solvents can dehydrate the nail and likely decrease the nail permeability. The transport of charged species across the nail can be modeled as hindered aqueous pore transport (18). The nail permselectivity to charged species is thus expected to be manipulated by changing the ionic strength of the delivery system. Understanding such manipulations may prove instrumental in transungual drug delivery development and specifically in delivering ionic drugs with low aqueous solubilities (i.e., low solution ionic strength).

Chemical and physical enhancement techniques have been investigated to improve transungual transport. Mercaptan compounds and keratolytic agents were shown to irreversibly degrade the nail thereby augmenting both hydration and transungual diffusion of model permeants (19,20). Electrically-assisted transport is similarly effective. Prednisolone was iontophoretically delivered across nail *in vivo* (21). In a separate study, salicylic acid was delivered across nail *in vitro*. The iontophoretic flux of salicylic acid increased with its concentration and was influenced by the ionic strength. The optimal ionic strength was between 50 and 100 mM (22). Using the neutral compounds mannitol and urea as well as charged tetraethylammonium bromide, electromigration was shown to be the dominant mechanism for transungual iontophoresis (18). The

[1] Division of Pharmaceutical Sciences, James L. Winkle College of Pharmacy, University of Cincinnati, Cincinnati, Ohio 45267, USA.
[2] To whom correspondence should be addressed. (e-mail: kevin.li@uc.edu)

0724-8741/09/0600-1446/0 © 2009 Springer Science + Business Media, LLC

contribution of electroosmosis was small, accounting for less than 10% of the overall iontophoretic transport enhancement for small ions. Increasing or decreasing the pH from the isoelectric point of the nail was shown to enhance electroosmotic transport (18,23,24), and electroosmosis could further be enhanced by decreasing the ionic strength of the system from 0.7 to 0.04 M (18,23). These findings provide the mechanistic framework in the development of transungual iontophoretic drug delivery to treat nail diseases. To date, the feasibility of iontophoretically enhanced delivery of terbinafine (25) and ciclopirox (26) over passive delivery into and across the nail have been demonstrated.

The present work investigated the effects of ionic strength on transungual transport. Specifically, the effects of ionic strength on passive and anodal iontophoretic transport across hydrated nail plate were examined with a model cationic permeant, tetraethylammonium ion (TEA). TEA was chosen as the model permeant because of its high water solubility that allowed the experiments of high ionic strength, its pH independent single positive charge, and its established free aqueous diffusion coefficient and hydration radius. The effects of ionic strength were first determined under symmetric conditions in which the donor and receiver solutions had the same ionic strength. Iontophoresis under asymmetric conditions (varying donor ionic strength with the receiver maintained at the physiological ionic strength) was then performed to mimic *in vivo* conditions. Prior to the transport studies, TEA uptake studies were carried out to assess partitioning of TEA into the nail. Hydration studies were also performed to determine the effect of ionic strength on nail hydration and integrity.

MATERIALS AND METHODS

Materials

Phosphate buffered saline (PBS) of pH 7.4 was prepared by dissolving PBS tablets (0.01 M phosphate buffer, 0.0027 M potassium chloride, and 0.137 M sodium chloride) obtained from Sigma-Aldrich (St. Louis, MO) in distilled, deionized water. Tetraethylammonium chloride (TEACl) solution was prepared by reacting tetraethylammonium hydroxide (20% *w*/*w*, Acros, Morris Plains, NJ) with hydrochloric acid or by dissolving tetraethylammonium chloride salt (99% purity, water content of 10% *w*/*w*, Acros, Morris Plains, NJ) in distilled, deionized water and subsequently adjusting the pH to 7.4. Sodium azide (99% purity, Acros, Morris Plains, NJ) was added at 0.02% to all solutions to inhibit bacterial growth; sodium azide content was considered in the ionic strength calculations. ^{3}H-mannitol (1–^{3}H(N)–, 10–30 Ci/mmol) and ^{14}C-tetraethylammonium bromide (1–^{14}C, 1–5 mCi/mmol) were purchased from PerkinElmer Life and Analytical Sciences (Boston, MA). The radiolabeled chemicals had a purity of at least 97%. All materials were used as received.

Preparation of Nail Samples

Frozen, cadaver human fingernails (male and female, age 24–90) were acquired from ScienceCare Anatomical (Phoenix, AZ). Prior to use, the nails were thawed in PBS at room temperature and cleaned by removing any residual tissues using forceps. Scraping and coloration were used as indicators to determine if the integument had been completely detached. The free edge and the cuticle end of the nails were trimmed as needed for smoothness and fit within the diffusion cells. The nails were then rinsed thoroughly with and soaked in PBS for at least 24 h to allow complete hydration before transport experiments. Nail clippings were obtained from healthy volunteers (male and female, age 23–50) using nail clippers. The nail clippings were cleaned with forceps, rinsed with PBS, and left to air dry overnight. The nail thicknesses ranged from 0.5 to 0.8 mm as measured using a micrometer (Mitutoyo, Kawaskai, Kanagawa, Japan). The use of human tissues was approved by the Institutional Review Board at the University of Cincinnati, Cincinnati, OH.

Hydration Studies

The nail hydration studies were divided into three stages. In Stage I, clean nail clippings were weighed and soaked in 1 mL of TEACl solution (0.02, 0.05, and 0.15 M) in a sealed scintillation vial. After hydration for 3 days (Stage IA), the nail clippings were removed, blotted dry with Kimwipes®, and quickly weighed (i.e., wet weight). The nail clippings were then hydrated for 11 days, removed from the TEAC1 solution, blotted dry, and weighed (Stage IB)—similar procedure as Stage IA. Subsequently, the nail clippings were dried in a 60°C oven overnight until a constant weight was achieved (i.e., dry weight). The percentage water content in the nail clippings (%WC) was expressed as the ratio of the difference between wet and dry weights ($\text{weight}_{\text{wet}}$ and $\text{weight}_{\text{dry}}$, respectively) divided by the dry weight multiplied by 100%:

$$\%\text{WC} = \frac{\text{weight}_{\text{wet}} - \text{weight}_{\text{dry}}}{\text{weight}_{\text{dry}}} \times 100\% \qquad (1)$$

Stages II and III were designed to check the integrity of the nails after treatment with the TEACl solutions in Stage I. Immediately after Stage I, the nail clippings were immersed in 1 mL aliquots of 0.15 M PBS for 48 h in Stage II. After removal from this solution, the nails were blotted dry, weighed, and oven dried overnight. Stage III was performed 2 weeks after Stage II and had the same procedure as Stage II. Water contents were determined using Eq. 1. The hydration studies in all stages were performed at room temperature (20±2°C).

Uptake Studies

Clean nail clippings were weighed and equilibrated in 3 mL of aqueous solutions spiked with 5 μL ^{14}C-TEA for 48 h at room temperature. TEACl and NaCl solutions of various ionic strengths (e.g., 0.01, 0.02, 0.03, 0.05 0.15, and 0.6 M) were used. After equilibration, the clippings were removed from the solution and blotted dry with Kimwipes®. The nail clippings were then immersed in 1 mL 0.15 M PBS to extract the permeant from the clippings. Twenty-four hours later, the nail clippings were removed from the extraction solution and transferred to fresh 0.15 M PBS for a second extraction. A third extraction was not carried out because the second extraction generally showed less than 5% of the amount in the first extraction. Ten milliliters of liquid scintillation cocktail (Ultima Gold™, PerkinElmer Life and Analytical Sciences, Shelton, CT) were added to each extraction solution

and the samples were assayed by a liquid scintillation counter (Beckman Counter LS6500, Fullerton, CA). Twenty microliters of equilibration solution were also withdrawn and mixed with 1 mL PBS and 10 mL liquid scintillation cocktail for liquid scintillation counting. The partition coefficient (K_{eff}) was calculated and expressed as the ratio of the amount of permeant per gram solution within the nail clippings to the amount of permeant per gram bulk solution:

$$K_{eff} = \frac{A_{Total} \Big/ \left(\text{weight}_{wet} - \text{weight}_{dry}\right)}{C_{eq}} \quad (2)$$

where A_{Total} is the total amount of TEA extracted and C_{eq} is the weight/weight concentration of TEA in the equilibrating solution.

Transport Studies

As shown in Table I, seven multi-stage treatment protocols were performed implementing a dual permeant strategy (concomitant MA and TEA delivery) as described in the literature (18,19,23). Testing the same nail and using it as its own control reduces inter-sample variability.

Treatment protocols 1 to 3 were passive transport studies. Each passive protocol included six stages in which the human nail plates were treated on both sides with solutions of varying ionic strengths (0.01, 0.03, 0.15, and 0.6 M). The data from the first passive stage (Stage I) in all protocols, in which the donor and receiver solutions were 0.15 M PBS, were not analyzed. This stage was precautionary—ensuring complete hydration of the nail plate. Stages II and VI, in which the

Table I. Treatment Protocols in the Nail Transport Studies for Mannitol (MA) and Tetraethylammonium Ion (TEA)

	Delivery method	Donor	Receiver
Treatment 1			
Stage I	Passive diffusion	0.15 M PBS	0.15 M PBS
Stage II	Passive diffusion	0.01 M PBS	0.01 M PBS
Stage III	Passive diffusion	0.03 M PBS	0.03 M PBS
Stage IV	Passive diffusion	0.15 M PBS	0.15 M PBS
Stage V	Passive diffusion	0.6 M PBS	0.6 M PBS
Stage VI	Passive diffusion	0.01 M PBS	0.01 M PBS
Treatment 2			
Stage I	Passive diffusion	0.15 M TEACl	0.15 M PBS
Stage II	Passive diffusion	0.01 M TEACl	0.01 M PBS
Stage III	Passive diffusion	0.03 M TEACl	0.03 M PBS
Stage IV	Passive diffusion	0.15 M TEACl	0.15 M PBS
Stage V	Passive diffusion	0.6 M TEACl	0.6 M PBS
Stage VI	Passive diffusion	0.01 M TEACl	0.01 M PBS
Treatment 3			
Stage I	Passive diffusion	0.15 M TEACl	0.15 M PBS
Stage II	Passive diffusion	0.01 M TEACl	0.15 M PBS
Stage III	Passive diffusion	0.03 M TEACl	0.15 M PBS
Stage IV	Passive diffusion	0.15 M TEACl	0.15 M PBS
Stage V	Passive diffusion	0.6 M TEACl	0.15 M PBS
Stage VI	Passive diffusion	0.01 M TEACl	0.15 M PBS
Treatment 4			
Stage I	Passive diffusion	0.15 M TEACl	0.15 M PBS
Stage II	Anodal iontophoresis	0.15 M TEACl	0.15 M PBS
Stage III	Anodal iontophoresis	0.02 M TEACl	0.15 M PBS
Stage IV	Anodal iontophoresis	0.02 M TEACl	0.02 M PBS
Stage V	Anodal iontophoresis	0.15 M TEACl	0.15 M PBS
Treatment 5			
Stage I	Passive diffusion	0.15 M TEACl	0.15 M PBS
Stage II	Anodal iontophoresis	0.15 M TEACl	0.15 M PBS
Stage III	Anodal iontophoresis	0.05 M TEACl	0.15 M PBS
Stage IV	Anodal iontophoresis	0.05 M TEACl	0.05 M PBS
Stage V	Anodal iontophoresis	0.15 M TEACl	0.15 M PBS
Treatment 6			
Stage I	Passive diffusion	0.15 M TEACl	0.15 M PBS
Stage II	Anodal iontophoresis	0.02 M TEACl	0.15 M PBS
Stage III	Anodal iontophoresis	0.02 M TEACl	0.02 M PBS
Stage IV	Anodal iontophoresis	0.02 M TEACl	0.15 M PBS
Treatment 7			
Stage I	Passive diffusion	0.15 M TEACl	0.15 M PBS
Stage II	Anodal iontophoresis	0.02 M TEACl	0.02 M PBS
Stage III	Anodal iontophoresis	0.02 M TEACl	0.15 M PBS
Stage IV	Anodal iontophoresis	0.02 M TEACl	0.02 M PBS

donor solutions were 0.01 M PBS in Treatment 1 and 0.01 M TEACl in Treatment 2, were the control stages to determine the stability of the nail. In the experiments, the donor solutions were PBS (Treatment 1) or TEACl (Treatments 2 and 3) spiked with 2 μCi of ^{3}H-MA and 1 μCi of ^{14}C-TEA. The receiver solutions in Treatments 1 and 2 were PBS and matched the ionic strength of the donor. In Treatment 3, the receiver solutions were always 0.15 M PBS. Treatment 1 was compared to Treatment 2 to examine the diffusion potential effect and effects due to the different diffusivities of TEA in the donor and Na^+ ion in the receiver (27).

Treatment protocols 4 to 7 were iontophoretic transport experiments. Treatment protocols 4 and 5 had five stages: a passive stage, two iontophoretic control stages, an asymmetric iontophoretic test stage, and a symmetric iontophoretic test stage. Control stages (Stages II and V), in which the donor was 0.15 M TEACl and the receiver was 0.15 M PBS, were used to determine the stability of the nail. The donor solutions in the test stages (Stages III and IV) were 0.02 M TEACl in Treatment 4 and 0.05 M TEACl in Treatment 5. All donor solutions were spiked with 2 μCi of ^{3}H-MA and 1 μCi of ^{14}C-TEA. The receiver solutions were 0.02, 0.05, and 0.15 M PBS. Note that the ionic strength range differs between passive and iontophoretic transport experiments; extreme ionic strength conditions were not studied for anodal iontophoretic delivery because a solution of 0.01 M ionic strength cannot provide the ions required to carry the electric current for 6 h and 0.6 M ionic strength is well above antifungal agent solubilities in aqueous media in general (28). During control and symmetric stages, the ionic strengths of the donor and receiver were matched. During the asymmetric stage, the receiver solution was always 0.15 M PBS. As the 0.02 M nail study generated less than expected reproducible results, additional replicates were performed (Treatments 6 and 7). Specifically, a third multistage protocol including either two 0.02 M asymmetric separated by a 0.02 M symmetric iontophoretic stage in Treatment 6 or two 0.02 M symmetric separated by a 0.02 M asymmetric iontophoretic stage in Treatment 7 was employed. Similar to the passive transport study, the data from the first passive stage (Stage I) in all treatment protocols were not included in the analyses.

In the experiments, excised nail plates were mounted between side-by-side diffusion cells with a compartmental volume of 2 mL (Dana Enterprise, West Chester, OH). The nails were secured using custom-made silicone adaptors (MED-6033, NuSil Silicone Technology, Carpinteria, CA) such that the dorsal side of the nail faced the donor chamber. Preliminary studies showed no noticeable permeant-to-adaptor binding. Both the half cells and the adaptors had an effective diffusion area of 0.64 cm^2.

A direct current of 0.1 mA was applied across the nail using a constant current device (Phoresor II Auto, Model PM 850, Iomed, Inc., Salt Lake City, UT) driven by Ag and Ag/AgCl electrodes in all iontophoresis stages. The anode was in the donor and the cathode was in the receiver. To maintain a constant permeant concentration in the donor, the donor solution was replaced with fresh donor solution every 6 h for the 0.02 M condition and every 12 h for the 0.05 and 0.15 M conditions. The voltage drop across the nail plate was measured at 0.1 mA using a mutlimeter (Fluke 73III, Everett, WA) to determine the nail resistance before and after each protocol and throughout iontophoresis.

Samples were withdrawn at predetermined time intervals. Ten microliters were removed from the donor compartment. One milliliter was removed from the receiver compartment with the replacement of fresh solution. Ten milliliters of liquid scintillation cocktail were added to each sample vial and the samples were assayed by the liquid scintillation counter. The cumulative amount of permeant delivered across the nail (Q) was plotted against time (t). The steady-state flux (J) was calculated using the slope of the linear portion of this curve, correcting for the diffusion area (A):

$$J = \frac{\Delta Q}{A\Delta t} \tag{3}$$

Passive experiments were 48 h long; iontophoretic delivery was 36 h. Eighteen to 36 h elapsed between stages during which the diffusion cells were rinsed three to five times and the nails were allowed to equilibrate in the solution of the upcoming stage. Constant stirring and room temperature (20±2°C) were maintained during all stages and equilibration periods.

Statistical Analysis

Stability was assessed by reproducibility between control stages. Specifically, nails were removed from the analysis if more than a two-fold difference was observed between the results in the control stages. In data analysis, the two-tailed t-test was used to evaluate the significance of the donor system (PBS *versus* TEACl) on TEA transport. The pooled test statistic was used because the standard deviations between the tested systems were statistically equivalent per the two-standard deviation F-test, which assumes simple random samples, independent samples, and a normal distribution. Two-tailed paired t-tests were used to evaluate the significance of ionic strength on TEA transport. Specifically, the two-way ANOVA model was implemented by executing the proc GLM function in SAS. Differences were considered significant at a level of $p<0.05$.

THEORY AND EQUATIONS

The effective partition coefficient of a permeant into the nail (K_{eff}) can be described by the product of the partition coefficient due to charge–charge interactions (K_e) and the partition coefficient related to other permeant-to-nail interactions such as size exclusion in the transport pathway (K_H).

$$K_{\text{eff}} = K_H K_e \tag{4}$$

Assuming the nail follows an aqueous pore pathway model and the pores are cylindrical, K_H can be expressed as:

$$K_H = K_p\left(1 - R_s/R_p\right)^2 \tag{5}$$

where $(1-R_s/R_p)^2$ is the size exclusion factor related to the hydration radius of the permeant R_s and the effective pore radius R_p, and K_p is the correction factor for partitioning due to effects such as hydrogen bonding and hydrophobic interactions. The K_e of a positively charged ion into a

negatively charged membrane is related to the charge of the ionic species i (z_i) and the surface charge density of the pore (σ) which is assumed to be uniform across the wall of the cylinder pore. K_e can be expressed as a function of the pore electrical potential ($\psi(r)$) integrated over the radial position in the pore (r) according to (29):

$$K_e = \frac{2}{(R')^2} \int_0^{R'} r \exp[-z_i e \psi(r)/kT] dr \quad (6)$$

where R' is the effective radius of the pore, e is the electronic charge, k is the Boltzmann constant, and T is the absolute temperature.

The electrical potential $\psi(r)$ due to charge–charge interactions between the ions and the ionic species of interest within a double layer along the pore wall is obtained from the Poisson–Boltzmann equation (29,30). The inner or Stern layer of the double layer contains tightly bound ions to the pore wall while the outer or diffuse region possesses less firmly bound ions. The electrical properties of this diffuse region—the electrical double layer—are controlled by the surface charge density of the pore wall as well as the ionic strength of the solution within the pore (29,31,32). The thickness of the electrical double layer is related to the ionic strength of the solution (I) by (23):

$$\kappa = \left(\frac{2F^2 I}{\varepsilon R_{gas} T} \right)^{1/2} \quad (7)$$

where R_{gas} is the gas constant, ε is the permittivity, and F is the Faraday constant. The ionic strength is related to the summation of the products of the molar concentration of the ions within the solution (c_j) and the square of the charge number of the respective ions (z_j),

$$I = \frac{1}{2} \sum c_j z_j^2 \quad (8)$$

Under low ionic strength conditions, the double layer thickness ($1/\kappa$) exceeds the pore radius (R_p), which in the case of nail is approximately 0.7 nm (18). Accordingly, κR_p is less than one at ionic strength below 0.15 M and the electrical potential in the pore ($\psi(r)$) can be assumed equivalent to $\psi(0)$. Note that, under this condition, pore geometry becomes somewhat irrelevant. $\psi(0)$ is a function of the surface charge density and the electrical double layer thickness and can be expressed as (30):

$$\psi(0) = \frac{\kappa^{-1}\sigma}{\varepsilon} \quad (9)$$

Assuming $\psi(r)=\psi(0)$ and substituting $\psi(0)$ from Eq. 9 into Eq. 6, followed by integration gives

$$K_e = e^{-\frac{\pi r}{kT}\left(\frac{\sigma}{\varepsilon\kappa}\right)} \quad (10)$$

Therefore, the logarithm of the partition coefficient is proportional to the thickness of the double layer, $1/\kappa$. Above 0.1 M ionic strength, the electrical potential $\psi(r)$ can no longer be assumed equal to $\psi(0)$ but decreases from $\psi(0)$ to a smaller value from at the pore wall to the center of the pore. Accordingly, at higher ionic strengths, K_e will be smaller than the values predicted by Eq. 10.

The permeability coefficient (P) related directly to the effective diffusion coefficient (D_{eff}) and effective partition coefficient (K_{eff}) of the permeant as given below:

$$P = \frac{J}{C_D} = \frac{D_{eff} K_{eff}}{h} = \frac{\varepsilon_p D_i D_H K_e K_H}{h} \quad (11)$$

where C_D is the concentration of the permeant in the donor chamber, h is the membrane thickness, ε_p is the combined porosity and tortuosity factor for the membrane (porosity divided by tortuosity), D_i is the free diffusion coefficient in solution, and D_H describes the hydrodynamic part of the hindered transport factor for Brownian diffusion defined previously (33). Taking the natural logarithm of Eq. 11:

$$\ln P = \ln \frac{\varepsilon_p D_i D_H K_H}{h} + \ln K_e \quad (12)$$

For electrically-assisted delivery of charged permeants, the efficiency of iontophoresis is associated with the transference number (t_i) and is given experimentally in terms of the iontophoretic flux ($J_{\Delta\psi,i}$), charge number, and the current density applied (I_c) (34):

$$t_i = \frac{|z_i| F J_{\Delta\psi,i}}{I_c} \quad (13)$$

Equation 13 can also be written in terms of the effective mobilities of the ionic species of interest, i, and of all ions in the membrane, j, (u_i and u_j, respectively) and their concentrations within the system (c_i and c_j, respectively) (34):

$$t_i = \frac{c_i u_i |z_i|}{\sum_j c_j u_j |z_j|} \quad (14)$$

RESULTS

Ionic Strength Effects on Nail Hydration and Integrity

Fig. 1 shows the results in the nail hydration experiments. Based on previous data, the average water content of control

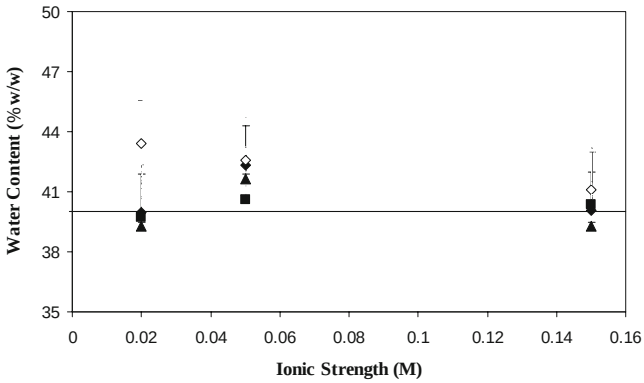

Fig. 1. Percentage water content in nail clippings treated with aqueous solutions of TEACl at various ionic strengths (0.02, 0.05, and 0.15 M). Data represent the mean and standard deviation of three nail samples. *Symbols*: Stage IA (*closed diamonds* and a *thick solid line*), Stage IB (*open diamonds* and a *dashed line*), Stage II (*closed squares* and a *dotted line*) Stage III (*closed triangles* and a *thin solid line*). The horizontal line is the average percentage water content in control nail clippings (fully hydrated at physiologic ionic strength and pH) previously established by Hao *et al.* (19) to be 40±6% where n=6.

nail clippings in 0.15 M PBS was 40±6% (19) and was essentially the same as those in 0.04 and 0.7 M PBS (23). Similar results of nail water content were obtained when the nails were equilibrated in 0.02, 0.05, and 0.15 M TEACl. These results suggest that the solution ionic strength did not affect nail hydration and that any differences observed in permselectivity in the transport experiments should not be due to changes in nail hydration. TEACl at the ionic strengths studied did not significantly affect the integrity of the nail as inferred from the similar water content results obtained throughout all three stages over the course of 1 month.

Ionic Strength Effects on Partitioning into the Nail

Fig. 2 presents the effective partition coefficients for TEA into the nail at various ionic strengths of TEACl solution. The effective nail partition coefficients of TEA at various ionic strengths of PBS are also presented in the figure. The data show that the effective partition coefficient for TEA was approximately 2.8 when the ionic strength of the equilibrating solution was around 0.01 to 0.02 M. The partition coefficient decreased approximately 30% when the ionic strength increased from 0.01 to 0.05 M. Further increases in the ionic strength of the solution to 0.15 M and ultimately 0.6 M resulted in a further decline in the partition coefficient. A comparison of the results from the experiments conducted in TEACl solution and PBS shows no significant difference between the two electrolyte systems and suggests no significant binding of TEA to the nail that would alter the surface charge in the nail and the charge–charge interactions between the nail and the permeant. The similar results in TEACl and PBS also suggest that TEA was as accessible as Na^+ ion to penetrate the nail to provide the same Debye–Huckel layer microenvironment for cation partitioning into the nail.

Effective Surface Charge Density of the Nail

To analyze the data using Eqs. 4 and 10, $\ln(K_{eff})$ was plotted against $I^{-1/2}$ in Fig. 3. The linear relationship between $\ln(K_{eff})$ and $I^{-1/2}$ suggests that the partitioning of the permeant into hydrated nail at physiological pH is consistent with the negatively charged aqueous pore model. The linear regression in Fig. 3 does not include the data point at 0.6 M, which falls outside the κR_p range assumed in the derivation of Eq. 10. As expected, the K_{eff} value at 0.6 M was lower than that predicted from the linear regression line in the figure, mostly due to the lower electrical potential ($\psi(r)$) in the pore away from the surface of the pore wall under the 0.6 M ionic strength condition. The effective surface charge density of the nail (σ) calculated from the slope of the plot was 5.9×10^{-3} C/m^2 (negative charge) and the K_H calculated from the y-intercept was 1.1. This surface charge density approximation is analogous to that ($\sim10^{-4}$ to 10^{-3} C/m^2) calculated previously (23). The difference between the present and previously determined values can be due to the limitation of the equation used in the electroosmosis calculation and possible different domains in the nail probed by the present uptake and previous electroosmosis methods—electroosmotic transport mainly probing the negatively charged transport pathway while uptake experiment studying the average properties of the whole nail plate. Experimental errors can also contribute to this difference. The slightly larger than unity K_H value suggests constant permeant partitioning due to non-ionic interactions independent of solution ionic strength (Eq. 5). This effect (K_p) leads to a greater than twofold solution-to-nail partitioning as previous effective pore size results of the nail transport pathway (18) indicated that $(1-R_s/R_p)^2$ was <0.4.

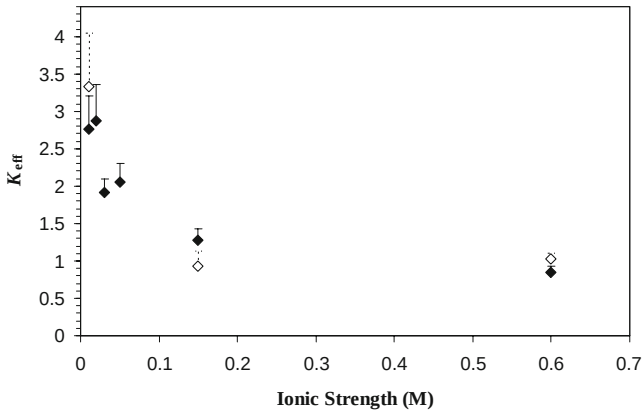

Fig. 2. The effective partition coefficient (K_{eff}, amount/g solution in nail divided by amount/g bulk TEACl) of TEA into nail clippings in TEACl solution of various ionic strengths (*closed diamond*, *solid line*) or PBS of various ionic strengths (*open diamond*, *dashed line*). Data represent the mean and standard deviation of three–four nail samples.

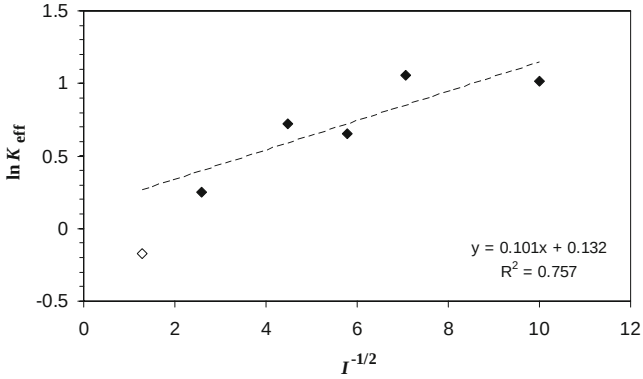

Fig. 3. Ionic strength effects on partitioning of TEA into the nail in TEACl solutions. The natural log values of the effective partition coefficients (ln K_{eff}) were plotted against the reciprocal square roots of the ionic strength ($I^{-1/2}$) of the bulk solution. *Closed diamonds*: ionic strengths within the κR_p limit of the theoretical equation assumption; *open diamond*: above this limit. Data represent the mean of four nail samples.

Ionic Strength Effects on Passive Transport Across the Nail

Fig. 4 shows the effects of the ionic strength on the passive permeability coefficient of the nail for TEA. The analysis was based on normalizing the permeability coefficients by the average 0.01 M permeability coefficient (Stages II and VI) to examine the change in nail permeability with increasing ionic strength. Under the symmetric conditions (Treatments 1 and 2) in which both the donor and receiver have the same ionic strength, TEA permeability was inversely related to ionic strength with the permeability of TEA at 0.01 M ionic strength significantly greater than those under the higher ionic strength conditions. A drop in TEA

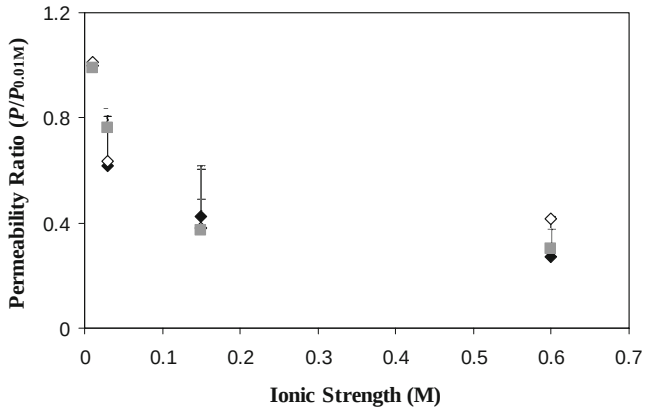

Fig. 4. Ionic strength effects on passive TEA permeability. Normalized passive permeability coefficients ($P/P_{0.01\ M}$) of TEA transport across nail: under symmetric conditions in which PBS was in both the donor and receiver in Treatment 1 (*closed diamonds*, *solid line*), under symmetric conditions in which TEACl was in the donor and PBS was in the receiver in Treatment 2 (*open diamonds*, *dashed line*), under asymmetric conditions in Treatment 3 (*squares*, *dotted line*). Data represent the mean and standard deviation of four nail samples. The permeability coefficients of the control stages at 0.01 M PBS in both the donor and receiver, 0.01 M TEACl in the donor and 0.01 M PBS in the receiver, and 0.01 M TEACl in the donor and 0.15 M PBS in the receiver were $4.4\times10^{-7}\pm3.4\times10^{-7}$, $4.8\times10^{-7}\pm2.1\times10^{-7}$, and $1.5\times10^{-7}\pm0.7\times10^{-7}$ cm/s, respectively (mean ± SD).

permeability occurred at 0.03 M compared with 0.01 M. The permeability further decreased when 0.15 M was used. At ionic strength greater than 0.15 M, the permeability coefficient approached a constant value after which ionic strength no longer impacted the permeability. Statistically similar results were obtained when PBS and TEACl systems were used in the donor compartment. No significant increase in the transport of TEA due to the permeation of the higher diffusivity Na^+ ion from the receiver to the donor (35) and the diffusion potential across the nail was observed. Under the asymmetric conditions (Treatment 3), a similar relationship between TEA permeability and ionic strength was observed. The ionic strength in the receiver at 0.15 M did not significantly alter the effects of ionic strength upon TEA permeation under the experimental conditions in the present study.

Being a neutral compound, MA should passively diffuse across the nail at a constant flux regardless of the ionic strength of the solutions. Graphically, this would be seen as a horizontal plot of permeability coefficients *versus* ionic strength. In the present study, the permeability coefficients for MA fluctuated between $1.6\times10^{-7}\pm0.8\times10^{-7}$ and $2.3\times10^{-7}\pm1.7\times10^{-7}$ cm/s under the various ionic strength conditions in Treatments 1 to 3. Due to these results, the MA data has henceforth been excluded from further analysis in the present study.

Effective Surface Charge Density of the Transport Pathway in the Nail

The effective surface charge density of the transport pathway in the hydrated nail plate was determined using the transport data obtained under the symmetric conditions and Eq. 12. Fig. 5 is a plot of $\ln P$ vs $I^{-1/2}$ using the average values in the passive transport experiments under the symmetric conditions in Treatments 1 and 2. The effective surface charge density (negative charge) estimated from the slope of this plot, 5.9×10^{-3} C/m^2, was essentially the same as that calculated using the partitioning data (Fig. 3) as the slopes in both plots are similar. This suggests that the transport pathway in the nail was essentially the same as the uptake domain probed in the partition experiment. It will also imply that the nail is relatively homogeneous in terms of its electrical charge properties in the uptake domain, passive transport pathway, and electroosmosis pathway. Thus, a single pathway model would likely be sufficient to describe transungual transport. The *y*-intercept in Fig. 5 is smaller but in the same order of magnitude as the value predicted by Eq. 12 assuming a nail transport pathway tortuosity of 4, using the free diffusion coefficient of 7×10^{-6} cm^2/s, and employing the parameters estimated from our previous studies (18,23): nail porosity of 0.4, hindered transport factor of 0.02, and nail thickness of 0.05 cm.

Ionic Strength Effects on Iontophoretic Transport Across the Nail

Fig. 6 shows the transference numbers of TEA across the hydrated nail plate in anodal iontophoresis under the symmetric and asymmetric ionic strength conditions. For iontophoretic transport in the symmetric system, the transference number of TEA (or iontophoresis efficiency) was related to the solution ionic strength. The relationship between transungual flux and ionic strength is similar to those in the passive transport experiments as the iontophoresis efficiency is a function of the product of effective diffusion coefficient (or electromobility) and concentration of TEA in the nail according to Eq. 14, which in turn is related to TEA partitioning into the nail due to charge-to-charge interactions (Eqs. 10 and 11). Under the asymmetric conditions, no significant ionic strength effect on the iontophoresis efficiency was observed and the transference number results did not differ from the control.

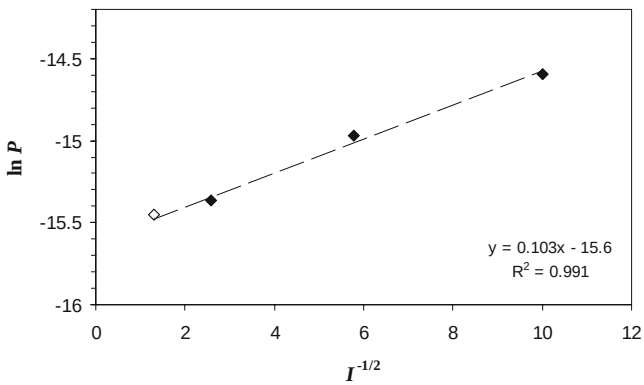

Fig. 5. Ionic strength effects on TEA passive permeability. The natural log values of the average permeability coefficients ($\ln P$) were plotted against the reciprocal square roots of the ionic strength ($I^{-1/2}$) of the bulk solution. The average P values in Treatments 1 and 2 are plotted. *Closed diamonds*: within the κR_p limit of the theoretical equation assumption; *open diamond*: above the limit. Data represent the mean of eight nail samples. Note that the linear regressions of the data in Treatments 1 and 2 are $y=0.089x-15.5$ and $y=0.117x-15.7$, respectively, not significantly different from the plot of the average data above.

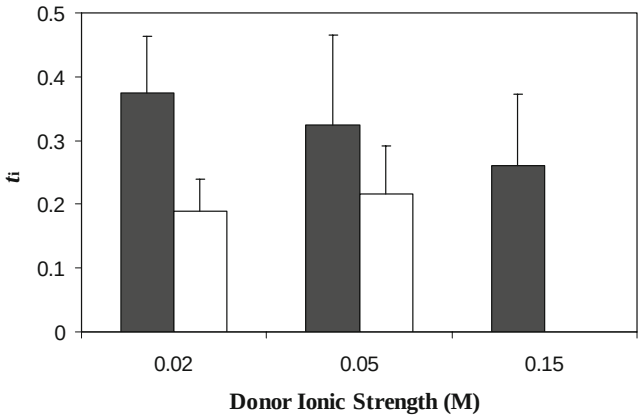

Fig. 6. Effects of ionic strength on transference number of TEA (t_i) across human nail under symmetric conditions (*closed bars*) and asymmetric conditions (*open bars*) in Treatments 4 to 7. In the symmetric system, the donor and receiver had the same ionic strength. In the asymmetric system, the receiver solution ionic strength was 0.15 M (donor solution did not match the receiver solution ionic strength). Data represent the mean and standard deviation of four–eight nail samples.

DISCUSSION

The degree of membrane permselectivity towards anions or cations depends upon the thickness of the electrical double layer within a pore and the pore radius. Therefore, the degree of membrane permselectivity is related to the ionic strength of the medium. The thickness of the electrical double layer is described by the Debye–Huckel reciprocal length and is inversely proportional to the square root of the ionic strength of the solution. Under high ionic strength conditions, the double layer extends minimally to the pore radial center and permselectivity is low—both cations and anions easily traverse the pore. As the ionic strength within the pore pathway decreases, the double layer thickens until the double layer thickness exceeds the pore radius ($1/\kappa > R_p$) and overlaps (29,31,32). Under such conditions, permselectivity would be significant and, for a negatively charged membrane, cations partition easily into the membrane while anions are excluded. Partitioning of cations into the negatively charged pores is increased at lower ionic strengths.

Better partitioning translates to higher permeability coefficients in both passive and iontophoretic transport (Eq. 11). This is consistent with the increase in partitioning and therefore the permeability of nail to the cationic permeant at low ionic strengths as observed in the present study. In general, the partitioning and passive transport results obtained in the present study are consistent with the electrokinetic theory and our proposed aqueous pore pathway model. Passive transport of neutral compounds is unaffected by the effect of double layer thickness and pore charge.

The extent of charge–charge interactions between the permeant and nail depends on the effective surface charge density of the pathways in the nail. It has been previously shown that the transport barrier of the nail is negatively charged. In the present study, the effective negative charge density of the nail was determined to be 5.9×10^{-3} C/m^2 at physiological pH, which is within the order of magnitude of that deduced from previous transungual electroosmosis data (23). Similar charge–charge interactions have been demonstrated in other biological systems such as the skin in transdermal delivery, in which ionic strength significantly influenced passive and iontophoretic transport (36,37).

Aside from partitioning, iontophoretic flux is dependent upon convective solvent flow and ion competition between TEA and the counterions (Cl^-) within the system during constant current iontophoresis. Although the contribution of electroosmosis to the system was shown to be small (18), the effects of ion competition can be considerable. Particularly, TEA competes with chloride ions which are smaller and exhibit higher electromobilities during iontophoresis. This effect can be magnified when the concentration of TEA in the donor and within the nail decreases (Eq. 14). In the asymmetric system, TEACl concentration and ionic strength gradients were established in the nail from the donor to receiver, and the larger the difference between the ionic strengths of the donor and receiver solutions, the steeper was the gradient. Therefore, the effect of ionic strength under the asymmetric conditions was expected to be smaller than the full effect under the symmetric conditions. As consequence of counterion competition and ionic strength gradient in the nail, the transference numbers for the low ionic strength asymmetric systems were one-half and two-thirds of their symmetric counterparts. As such, the flux of TEA across nail—when physiologic conditions were used in the receiver—was approximately the same at all ionic strengths studied.

The development of an effective topical transungual delivery system is challenging due to the strong barrier of the nail. Topical administration of antifungal agents is further inhibited by the low aqueous solubility of these agents. Organic solvents and solubilizing agents are commonly used to increase drug concentrations in formulations. These methods come with financial and practical costs. For instance, organic solvents can dehydrate the nail and reduce transungual permeation. There can also be side effects associated with these solvents/agents in the treatment. The ionic strength effect demonstrated in the present study suggests that positively charged drugs can effectively partition and transport into the nail at low aqueous concentrations at physiological pH. It also suggests that the disadvantage of delivering cationic drugs of low solubilities was not as significant due to enhanced partitioning of the drugs into the nail at low solution ionic strength.

CONCLUSION

The present study investigated the effects of solution ionic strength on nail partitioning and transungual passive and iontophoretic transport of a positively charged permeant at physiological pH. The integrity of the nail was also examined in the nail hydration experiments and was shown not to be affected by the ionic strengths studied. In the partitioning and transport experiments, when the ionic strength decreased, permeant partitioning into the nail and transport across the nail increased. This observation is consistent with electrokinetic theory and a negatively charged aqueous pore pathway model. In addition to quantifying the effects of solution ionic strength on the partitioning and transungual transport of the ionic permeant, the effective surface charge density of the transungual pathway in the nail

was determined. Together, these results provide mechanistic and practical insights into topical transungual delivery of ionic drugs. The results in the present study suggest that positively charged drugs can effectively partition into the nail at low donor concentration due to ion-to-nail charge interactions countering the effect of low drug concentration in the donor chamber of a drug delivery device upon flux.

ACKNOWLEDGMENTS

This research was supported by NIH Grant GM063559 and in part by a grant from Boehringer Ingelheim Cares Foundation for the thesis work of Kelly A. Smith.

REFERENCES

1. R. P. R. Dawber, D. A. R. deBerker, and R. Baran. Science of the nail apparatus. In R. Baran, R. P. R. Dawber, D. A. R. deBerker, E. Haneke, and A. Tosti (eds.), *Baran and Dawber's Diseases of the Nails and their Management*, Blackwell Science, Oxford, 2001, pp. 1–48.
2. R. P. R. Dawber, and R. Baran. Structure, embryology, comparative anatomy and physiology of the nail. In R. Baran, and R. P. R. Dawber (eds.), *Baran and Dawber's Diseases of the Nails and their Management*, Blackwell Science, Boston, 1984, pp. 1–23.
3. M. Gniadecka, O. Faurskov Nielsen, D. H. Christensen, and H. C. Wulf. Structure of water, proteins, and lipids in intact human skin, hair, and nail. *J. Invest. Dermatol.* **110**:393–398 (1998). doi:10.1046/j.1523-1747.1998.00146.x.
4. A. L. Lorincz, and R. B. Stoughton. Specific metabolic processes of skin. *Physiol. Rev.* **38**:481–502 (1958).
5. J. L. Marty. Amorolfine nail lacquer: a novel formulation. *JEADV.* **4**:S17–S21 (1995). doi:10.1016/0926-9959(94)00075-B.
6. B. Schulz, D. Chan, J. Backstrom, M. Rubhausen, K. P. Wittern, S. Wessel, R. Wepf, and S. Williams. Hydration dynamics of human fingernails: an ellipsometric study. *Phys. Rev. E Stat. Nonlin. Soft Matter Phys.* **65**:061913–1–061913-7 (2002).
7. R. I. C. Spearman. The physiology of the nail. In A. Jarrett (ed.), *The Physiology and Pathophysiology of the Skin, Vol. 5: The Sweat Glands, Skin, Permeation, Lymphatics, the Nails*, Academic, New York, 1973, pp. 1812–1853.
8. Y. Kobayashi, T. Komatsu, M. Sumi, S. Numajiri, M. Miyamoto, D. Kobayashi, K. Sugibayashi, and Y. Morimoto. *In vitro* permeation of several drugs through the human nail plate: relationship between physicochemical properties and nail permeability of drugs. *Eur. J. Pharm. Sci.* **21**:471–477 (2004). doi:10.1016/j.ejps.2003.11.008.
9. D. Mertin, and B. C. Lippold. *In-vitro* permeability of the human nail and of a keratin membrane from bovine hooves: prediction of the penetration rate of antimycotics through the nail plate and their efficacy. *J. Pharm. Pharmacol.* **49**:866–872 (1997).
10. D. Mertin, and B. C. Lippold. *In-vitro* permeability of the human nail and of a keratin membrane from bovine hooves: penetration of chloramphenicol from lipophilic vehicles and a nail lacquer. *J. Pharm. Pharmacol.* **49**:241–245 (1997).
11. D. Mertin, and B. C. Lippold. *In-vitro* permeability of the human nail and of a keratin membrane from bovine hooves: influence of the partition coefficient octanol/water and the water solubility of drugs on their permeability and maximum flux. *J. Pharm. Pharmacol.* **49**:30–34 (1997).
12. K. A. Walters, G. L. Flynn, and J. R. Marvel. Physicochemical characterization of the human nail: I. Pressure sealed apparatus for measuring nail plate permeabilities. *J. Invest. Dermatol.* **76**:76–79 (1981). doi:10.1111/1523-1747.ep12525318.
13. K. A. Walters, G. L. Flynn, and J. R. Marvel. Physicochemical characterization of the human nail: permeation pattern for water and the homologous alcohols and differences with respect to the stratum corneum. *J. Pharm. Pharmacol.* **35**:28–33 (1983).
14. K. A. Walters, G. L. Flynn, and J. R. Marvel. Physicochemical characterization of the human nail: solvent effects on the permeation of homologous alcohols. *J. Pharm. Pharmacol.* **37**:771–775 (1985).
15. K. A. Walters, G. L. Flynn, and J. R. Marvel. Penetration of the human nail plate: the effects of vehicle pH on the permeation of miconazole. *J. Pharm. Pharmacol.* **37**:498–499 (1985).
16. A. Srebrnik, S. Levtov, R. Ben-Ami, and S. Brennert. Liver failure and transplantation after itraconazole treatment for toenail onychomycosis. *JEADV.* **19**:205–207 (2005). doi:10.1111/j.1468-3083.2005.00943.x.
17. C. O. Wilson, J. H. Block, O. Gisvold, and J. M. Beale. Appendix, *Wilson and Gisvold's Textbook of Organic, Medicinal and Pharmaceutical Chemistry*. Lippincott Williams & Wilkins, Philadelphia, 2004, pp. 948–956.
18. J. Hao, and S. K. Li. Transungual iontophoretic transport of polar neutral and positively charged model permeants: effects of electrophoresis and electroosmosis. *J. Pharm. Sci.* **97**:893–905 (2008). doi:10.1002/jps.21025.
19. J. Hao, K. A. Smith, and S. K. Li. Chemical method to enhance transungual transport and iontophoresis efficiency. *Int. J. Pharm.* **357**:61–69 (2008). doi:10.1016/j.ijpharm.2008.01.027.
20. R. H. Khengar, S. A. Jones, R. B. Turner, B. Forbes, and M. B. Brown. Nail swelling as a pre-formulation screen for the selection and optimisation of ungual penetration enhancers. *Pharm. Res.* **24**:2207–2212 (2007). doi:10.1007/s11095-007-9368-3.
21. M. P. James, R. M. Graham, and J. English. Percutaneous iontophoresis of prednisolone—a pharmacokinetic study. *Clin. Exp. Dermatol.* **11**:54–61 (1986). doi:10.1111/j.1365-2230.1986.tb00424.x.
22. S. N. Murthy, D. E. Wiskirchen, and C. P. Bowers. Iontophoretic drug delivery across human nail. *J. Pharm. Sci.* **96**:305–311 (2007). doi:10.1002/jps.20757.
23. J. Hao, and S. K. Li. Mechanistic study of transungual electroosmosis transport across hydrated nail plates: effects of pH and ionic Strength. *J. Pharm. Sci.* **97**:5186–5197 (2008). doi:10.1002/jps.21368.
24. S. N. Murthy, D. C. Waddell, H. N. Shivakumar, A. Balaji, and C. P. Bowers. Iontophoretic permselective property of human nail. *J. Dermatol. Sci.* **46**:150–152 (2007). doi:10.1016/j.jdermsci. 2006.12.010.
25. A. B. Nair, S. R. Vaka, S. M. Sammeta, H. D. Kim, P. M. Friden, B. Chakraborty, and S. N. Murthy. Trans-ungual iontophoretic delivery of terbinafine. *J. Pharm. Sci.* (2009) in press. doi:10.1002/jps.21555.
26. J. Hao, K. A. Smith, and S. K. Li. Iontophoretically enhanced ciclopirox delivery into and across human nail plate. *J. Pharm. Sci.* (2009) in press. doi:10.1002/jps.21664.
27. S. K. Li, A. H. Ghanem, K. D. Peck, and W. I. Higuchi. Iontophoretic transport across a synthetic membrane and human epidermal membrane: a study of the effects of permeant charge. *J. Pharm. Sci.* **86**:680–689 (1997). doi:10.1021/js960479m.
28. D. S. Wishart, C. Knox, A. C. Guo, S. Shrivastava, M. Hassanali, P. Stothard, Z. Chang, and J. Woolsey. DrugBank: a comprehensive resource for in silico drug discovery and exploration. *Nucleic Acids. Res.* **34**:D668–D672 (2006). doi:10.1093/nar/gkj067.
29. S. M. Sims, W. I. Higuchi, V. Srinivasan, and K. D. Peck. Ionic partition coefficients and electroosmotic flow in cylindrical pores: comparison of the predictions of the Poisson–Boltzmann equation with experiment. *J. Colloid Interface Sci.* **155**:210–220 (1993). doi:10.1006/jcis.1993.1027.
30. P. C. Hiemenz, and R. Rajagopalan. The Electrical Double Layer and Double-Layer Interactions. In *Principles of Colloid and Surface Chemistry*. Marcel Dekker, New York, 1997, pp. 499–533.
31. R. Schmuhl, K. Keizer, A. van den Berg, J. E. ten Elshof, and D. H. A. Blank. Controlling the transport of cations through permselective mesoporous alumina layers by manipulation of electric field and ionic strength. *J. Colloid Interface Sci.* **273**:331–338 (2004). doi:10.1016/j.jcis.2003.10.024.
32. T. Kuo, L. A. Sloan, J. V. Sweedler, and P. W. Bohn. Manipulating molecular transport through nanoporous membranes by control of electrokinetic flow: effect of surface charge density and Debye length. *Langmuir.* **17**:6298–6303 (2001). doi:10.1021/la010429j.
33. W. M. Deen. Hindered transport of large molecules in liquid-filled pores. *AlChE J.* **33**:1409–1425 (1987).

34. J. B. Phipps, and J. R. Gyory. Transdermal ion migration. *Adv. Drug Deliv. Rev.* **9**:137–176 (1992). doi:10.1016/0169-409X(92)90022-I.
35. J. R. Vinograd, and J. W. McBain. Diffusion of electrolytes and of the ions in their mixtures. *J. Am. Chem. Soc.* **63**:2008–2015 (1941). doi:10.1021/ja01852a063.
36. K. D. Peck, A. H. Ghanem, W. I. Higuchi, and V. Srinivasan. Improved stability of the human epidermal successive permeability experiments. *Int. J. Pharm.* **98**:141–147 (1993). doi:10.1016/0378-5173(93)90050-P.
37. W. H. M. Craane-van Hinsberg, L. Bax, N. H. M. Flinterman, J. Verhoef, H. E. Junginger, and H. E. Bodde. Iontophoresis of a model peptide across human skin *in vitro*: effects of iontophoresis, protocol, pH, and ionic strength on peptide flux and skin impedance. *Pharm. Res.* **11**:1296–1300 (1994). doi:10.1023/A:1018994428375.